

An efficient split-step compact finite difference method for cubic–quintic complex Ginzburg–Landau equations[☆]

Shanshan Wang*, Luming Zhang

College of Science, Nanjing University of Aeronautics and Astronautics, Nanjing 210016, PR China



ARTICLE INFO

Article history:

Received 25 August 2011

Received in revised form

14 January 2013

Accepted 18 January 2013

Available online 4 February 2013

Keywords:

Cubic-quintic complex Ginzburg–Landau equation

Split-step method

Compact finite difference method

Runge–Kutta method

Multidimensional

ABSTRACT

We propose an efficient split-step compact finite difference method for the cubic–quintic complex Ginzburg–Landau (CQ CGL) equations both in one dimension and in multi-dimensions. The key point of this method is to separate the original CQ CGL equations into two nonlinear subproblems and one or several linear ones. The linear subproblems are solved by the compact finite difference schemes. As the nonlinear subproblems cannot be solved exactly, the Runge–Kutta method is applied and the total accuracy order is not reduced. The proposed method is convergent of second-order in time and fourth-order in space, which is confirmed numerically. Extensive numerical experiments are carried out to examine the performance of this method for the nonlinear Schrödinger equations, the cubic complex Ginzburg–Landau equation, and the CQ CGL equations. It is shown from all the numerical tests that the present method is efficient and reliable.

© 2013 Elsevier B.V. All rights reserved.

1. Introduction

The complex Ginzburg–Landau (CGL) models are studied extensively in chemistry, biology and especially in various branches of physics [1–3], such as superconductivity, superfluidity, nonlinear optics, Bose–Einstein condensation, etc. The cubic–quintic complex Ginzburg–Landau (CQ CGL) equation was introduced in [4] to seek two-dimensional (2D) solitary spiral solutions in active media with an excitation threshold. Ever since, numerous researches have investigated for this type of equation. For 1D, soliton solutions were constructed and analyzed both for the cubic CGL and the CQ CGL equations [5,6]. An analysis of 2D spiral solitons within the framework of the CQ CGL equation was developed in [7]. The Exp-function methods helped by symbolic computations of Maple were used to construct solitary and periodic solutions of the 2D CQ CGL equation [8]. The variational method was applied to obtain steady state solutions of the 1D, 2D, and 3D CQ CGL equations [9]. For 3D, stability of dissipative optical solitons in the CQ CGL equation were studied in [10], and collisions between stable solitons were presented in [11,12].

Though many studies of the exact solutions and their stabilities of the CQ CGL equations were made, analytical expressions of the exact solutions exist only for a few particular sets of parameters [9,13]. Analytical approximate methods might be used to describe features of soliton solutions, however, this works only for the most prominent features of solitons over a limited range of parameters [3]. Consequently, numerical solutions are necessary, and numerical simulations are also required to seek the complete features. The aim of this paper is to introduce an efficient numerical method for the CQ CGL equation both in one dimension and in multi-dimensions.

In this paper, we consider the d-dimensional ($d = 1, 2, 3$) cubic–quintic complex Ginzburg–Landau equation:

$$i\frac{\partial\psi(\mathbf{x}, t)}{\partial t} + (\alpha - i\beta)\Delta\psi(\mathbf{x}, t) + i\delta\psi + (\alpha_1 - i\beta_1)|\psi|^2\psi + (\alpha_2 - i\beta_2)|\psi|^4\psi = 0, \quad \mathbf{x} \in \mathbb{R}^d, t > 0, \quad (1)$$

where ψ is an unknown complex function, and α , β , α_1 , α_2 , β_1 , β_2 and δ are real parameters. When $\alpha_2 = \beta_2 = 0$, Eq. (1) is the cubic CGL equation. When $\beta = \delta = \beta_1 = \beta_2 = 0$, Eq. (1) is known as the cubic–quintic nonlinear Schrödinger (CQ NLS) equation [14,15]. If $\alpha_2 = 0$ in the CQ NLS equation, the usual cubic NLS equation results.

Various numerical studies have been made for the NLS equation, while split step methods attract more and more attention. Split step methods, also known as fractional step methods, are efficient and extensively used for numerical solutions of differential equations, especially for higher dimensional ones [16,17].

[☆] Foundation Item: This work was partly supported by the Talent Recruitment Foundation of Nanjing University of Aeronautics and Astronautics, No. 56YAH12021.

* Corresponding author.

E-mail addresses: wangss@nuaa.edu.cn (S. Wang), zhanglm@nuaa.edu.cn (L. Zhang).

Taha et al. [18] compare a split-step Fourier method with many other schemes for the 1D cubic NLS equation. Bao et al. [19,20] present the time-splitting spectral method and the time-splitting sine-spectral method for multi-dimensional Schrödinger equations. Wang [21] has applied the split-step finite difference (SSFD) method to solve various NLS equations in both one dimension and higher dimensions. Dehghan et al. [22] improve the SSFD method for the NLS equations with constant and variable coefficients by replacing the Crank–Nicolson scheme with a compact difference one. However, they consider the 1D problem. Goldman et al. [23] present a split-step Fourier algorithm for the d-dimensional cubic CGL equation. Zhang et al. [24] study the 2D Ginzburg–Landau–Schrödinger (GLS) equation by combining the split step approach with the Fourier pseudo-spectral method, the finite element method and the Crank–Nicolson scheme. Wang [25] introduces a split-step Chebyshev–Tau spectral method for the GLS equation. Degond et al. [26] study a time splitting spectral method for the cubic CGL equation in the large time and space limit. Xu et al. [27] propose three difference schemes for the 2D cubic CGL equation, one of which is a split-step finite difference scheme. Wainblat et al. [28] numerically analyze the collisions of dissipative solutions in the 2D CQ CGL equation by the split-step Fourier method, but they do not tell how to implement the method. Actually, special studies of split-step method itself for the CQ CGL equation are rare. The objective of this paper is to propose an efficient split-step compact finite difference method for the 1D, 2D, and 3D CQ CGL equations. Extensive numerical experiments are also carried out to test the efficiency of the method.

The remainder of this paper is arranged as follows. In Section 2, the split-step compact finite difference method is constructed for the CQ CGL equations. Numerical tests are discussed in Section 3, and some conclusions are drawn in Section 4.

2. Numerical method

For numerical computations, we consider the following initial-boundary value problem of the CQ CGL equation:

$$\begin{aligned} i \frac{\partial \psi(\mathbf{x}, t)}{\partial t} + (\alpha - i\beta) \Delta \psi(\mathbf{x}, t) + i\delta \psi + (\alpha_1 - i\beta_1) |\psi|^2 \psi \\ + (\alpha_2 - i\beta_2) |\psi|^4 \psi = 0, \quad (\mathbf{x}, t) \in \Omega_d \times (0, T], \end{aligned} \quad (2)$$

with the initial condition:

$$\psi(\mathbf{x}, 0) = \psi_0(\mathbf{x}), \quad \mathbf{x} \in \Omega_d, \quad (3)$$

and the homogeneous Dirichlet boundary conditions:

$$\psi(\mathbf{x}, t) = 0, \quad (\mathbf{x}, t) \in \partial \Omega_d \times [0, T], \quad (4)$$

or the periodic boundary conditions, where $\partial \Omega_d$ is the boundary of Ω_d .

2.1. Split-step method

First of all, second-order Strang splitting [17,29] is applied, so Eq. (2) is separated into three subproblems:

$$\begin{aligned} i \frac{\partial \psi(\mathbf{x}, t)}{\partial t} + \frac{1}{2} i\delta \psi + \frac{1}{2} (\alpha_1 - i\beta_1) |\psi|^2 \psi \\ + \frac{1}{2} (\alpha_2 - i\beta_2) |\psi|^4 \psi = 0, \end{aligned} \quad (5)$$

$$i \frac{\partial \psi(\mathbf{x}, t)}{\partial t} + (\alpha - i\beta) \Delta \psi(\mathbf{x}, t) = 0, \quad (6)$$

$$\begin{aligned} i \frac{\partial \psi(\mathbf{x}, t)}{\partial t} + \frac{1}{2} i\delta \psi + \frac{1}{2} (\alpha_1 - i\beta_1) |\psi|^2 \psi \\ + \frac{1}{2} (\alpha_2 - i\beta_2) |\psi|^4 \psi = 0. \end{aligned} \quad (7)$$

Hence, the process of solving Eq. (2) from t to $t + \Delta t$ can be replaced by solving Eqs. (5)–(7) within $[t, t + \Delta t]$, in sequence.

For $d = 1$, Eq. (6) is written as:

$$i \frac{\partial \psi}{\partial t} + (\alpha - i\beta) \frac{\partial^2 \psi}{\partial x^2} = 0. \quad (8)$$

For two dimensions, Eq. (6) is formulated as follows:

$$i \frac{\partial \psi}{\partial t} + (\alpha - i\beta) \left(\frac{\partial^2 \psi}{\partial x^2} + \frac{\partial^2 \psi}{\partial y^2} \right) = 0. \quad (9)$$

The first-order Lie formula [17] is used, and Eq. (9) could be split further into two 1D equations:

$$i \frac{\partial \psi}{\partial t} + (\alpha - i\beta) \frac{\partial^2 \psi}{\partial x^2} = 0, \quad (10)$$

$$i \frac{\partial \psi}{\partial t} + (\alpha - i\beta) \frac{\partial^2 \psi}{\partial y^2} = 0. \quad (11)$$

Since the two differential operators, i.e. $\partial^2/\partial x^2$ and $\partial^2/\partial y^2$, are commutable, the above splitting is exact with no error.

Similarly, Eq. (6) in 3D can be exactly separated as

$$i \frac{\partial \psi}{\partial t} + (\alpha - i\beta) \frac{\partial^2 \psi}{\partial x^2} = 0, \quad (12)$$

$$i \frac{\partial \psi}{\partial t} + (\alpha - i\beta) \frac{\partial^2 \psi}{\partial y^2} = 0. \quad (13)$$

$$i \frac{\partial \psi}{\partial t} + (\alpha - i\beta) \frac{\partial^2 \psi}{\partial z^2} = 0. \quad (14)$$

In conclusion, the total splitting error of the above process is second-order.

2.2. Numerical method for nonlinear subproblems

Let τ be the step size in time, such that $t_n = n\tau$, $n = 0, 1, 2, \dots, J$. Let ψ^n be the approximation of $\psi(\mathbf{x}, t_n)$.

Multiply Eq. (5) by ψ and take the imaginary part of the result. Then we obtain

$$\frac{\partial}{\partial t} |\psi|^2 = -\delta |\psi|^2 + \beta_1 |\psi|^4 + \beta_2 |\psi|^6. \quad (15)$$

If $\delta = \beta_1 = \beta_2 = 0$, it follows that $|\psi|^2$ is independent on t , i.e., $|\psi|^2 = |\psi^n|^2$. Thus, Eq. (5) can be integrated in time easily to obtain

$$\psi^* = \psi^n \exp \left[\frac{\tau}{2} (i\alpha_1 |\psi^n|^2 + i\alpha_2 |\psi^n|^4) \right]. \quad (16)$$

If $\delta = \beta_2 = 0$, Eq. (15) can be integrated from t_n to t , and one can get

$$|\psi|^2 = \frac{1}{\frac{1}{|\psi^n|^2} - \beta_1(t - t_n)}. \quad (17)$$

Set $\alpha_2 = 0$. It follows from Eq. (5) that

$$\psi^* = \psi^n \exp \left\{ -\frac{i\alpha_1 + \beta_1}{2\beta_1} \ln |1 - \beta_1 |\psi^n|^2(t - t_n)| \right\}. \quad (18)$$

If $\beta_2 = 0$, $\delta \neq 0$, Eq. (15) can be integrated from t_n to t . Thus,

$$\frac{|\psi|^2}{-\delta + \beta_1 |\psi|^2} = \frac{|\psi^n|^2}{-\delta + \beta_1 |\psi^n|^2} \exp[-\delta(t - t_n)]. \quad (19)$$

Therefore,

$$|\psi|^2 = \frac{\delta S}{(\beta_1 S - 1)}, \quad (20)$$

where

$$S = \frac{|\psi^n|^2}{-\delta + \beta_1 |\psi^n|^2} \exp[-\delta(t - t_n)]. \quad (21)$$

Suppose $\alpha_2 = 0$. It follows from Eq. (5) that

$$\psi^* = \psi^n \exp \left\{ -\frac{1}{2} \left(\tau \delta + \frac{i\alpha_1 + \beta_1}{\beta_1} \ln |1 - \beta_1 S| \right) \right\}. \quad (22)$$

The above sets of parameters correspond to the NLS equation and the cubic CGL equation, respectively. However, for the CQ CGL equation, it is difficult to obtain the analytical expression of $|\psi|^2$. Integrating Eq. (15) in time from t_n to t , by the help of symbolic computations of MATLAB, one obtains

$$\begin{aligned} & -\frac{1}{\delta} \ln |\psi|^2 + \frac{1}{2\delta} \ln(-\delta + \beta_1 |\psi|^2 + \beta_2 |\psi|^4) \\ & - \frac{\beta_1 \tanh^{-1} \left(\frac{\beta_1 + 2\beta_2 |\psi|^2}{\sqrt{4\delta\beta_2 + \beta_1^2}} \right)}{\delta \sqrt{4\delta\beta_2 + \beta_1^2}} \\ & = -\frac{1}{\delta} \ln |\psi^n|^2 + \frac{1}{2\delta} \ln(-\delta + \beta_1 |\psi^n|^2 + \beta_2 |\psi^n|^4) \\ & - \frac{\beta_1 \tanh^{-1} \left(\frac{\beta_1 + 2\beta_2 |\psi^n|^2}{\sqrt{4\delta\beta_2 + \beta_1^2}} \right)}{\delta \sqrt{4\delta\beta_2 + \beta_1^2}} + t - t_n, \end{aligned}$$

where \tanh^{-1} is the inverse hyperbolic tangent. Unfortunately, it is impossible to solve $|\psi|^2$ explicitly. Thus, the nonlinear subproblem (5) cannot be integrated exactly.

In fact, it is not necessary to solve Eq. (5) exactly, since the split-step approach is not exact with a splitting error of second-order. Moreover, the compact finite difference method for the linear subproblems, which is introduced in the next subsection, is also of second-order accuracy in time. Therefore, numerical solution is required and sufficient.

In this paper, we apply a second-order Runge–Kutta (RK) method [30] for solving the nonlinear equation (5) as follows:

$$\psi^* = \psi^n + \frac{\tau}{2}(K_1 + K_2), \quad (23)$$

$$K_1 = \frac{1}{2} [-\delta + (i\alpha_1 + \beta_1)|\psi^n|^2 + (i\alpha_2 + \beta_2)|\psi^n|^4] \psi^n, \quad (24)$$

$$\begin{aligned} K_2 &= \frac{1}{2} [-\delta + (i\alpha_1 + \beta_1)|\psi^n + \tau K_1|^2 \\ &+ (i\alpha_2 + \beta_2)|\psi^n + \tau K_1|^4] (\psi^n + \tau K_1). \end{aligned} \quad (25)$$

Eq. (7) is solved by the same approach. Actually, this approximate method is effective for Eqs. (5) and (7) with different sets of parameters. Even if the equations analyzed above could be solved exactly, the numerical approach is still comparable in accuracy to the exact solution. This issue is discussed in the section on numerical experiments.

2.3. Compact finite difference method for linear subproblems

A compact finite difference (CFD) method is utilized to solve the 1D linear equations, i.e. Eqs. (8) and (10)–(14). Suppose $\Omega_1 = [x_L, x_R]$, $\Omega_2 = [x_L, x_R] \times [y_L, y_R]$, $\Omega_3 = [x_L, x_R] \times [y_L, y_R] \times [z_L, z_R]$. Let h be the step size for the spatial grid, such that $x_j = x_L + jh$, $j = 0, 1, 2, \dots, N_x$, $y_k = y_L + kh$, $k = 0, 1, 2, \dots, N_y$, and $z_l = z_L + lh$, $l = 0, 1, 2, \dots, N_z$. Let ψ_j^n , ψ_{jk}^n and ψ_{jkl}^n be the approximations of $\psi(x_j, t_n)$, $\psi(x_j, y_k, t_n)$ and $\psi(x_j, y_k, z_l, t_n)$, respectively.

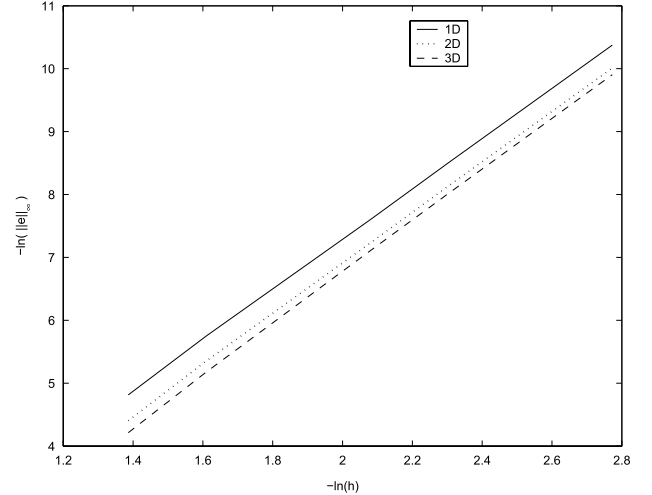


Fig. 1. Curves of convergence rates of the 1D, 2D, and 3D SSRKCFD schemes.

For $d = 1$, applying the Crank–Nicolson scheme for Eq. (8), one obtains

$$i \frac{\psi_j^{n+1} - \psi_j^n}{\tau} + \frac{1}{2}(\alpha - i\beta) \frac{1}{h^2} \delta_x^2 (\psi_j^{n+1} + \psi_j^n) = 0,$$

where

$$\delta_x^2 \psi_j^n = \psi_{j+1}^n - 2\psi_j^n + \psi_{j-1}^n.$$

Replace the second-order difference operator δ_x^2 by the compact one as follows:

$$\frac{\delta_x^2}{h^2 (1 + \frac{1}{12} \delta_x^2)}.$$

Then we obtain

$$\begin{aligned} & \left[i + \frac{i}{12} \delta_x^2 + \frac{1}{2}(\alpha - i\beta) \frac{\tau}{h^2} \delta_x^2 \right] \psi_j^{n+1} \\ &= \left[i + \frac{i}{12} \delta_x^2 - \frac{1}{2}(\alpha - i\beta) \frac{\tau}{h^2} \delta_x^2 \right] \psi_j^n. \end{aligned}$$

Consequently,

$$\begin{aligned} & \left[\frac{i}{12} + \frac{1}{2}(\alpha - i\beta) \frac{\tau}{h^2} \right] (\psi_{j+1}^{n+1} + \psi_{j-1}^{n+1}) \\ &+ \left[\frac{5i}{6} - (\alpha - i\beta) \frac{\tau}{h^2} \right] \psi_j^{n+1} \\ &= \left[\frac{i}{12} - \frac{1}{2}(\alpha - i\beta) \frac{\tau}{h^2} \right] (\psi_{j+1}^n + \psi_{j-1}^n) \\ &+ \left[\frac{5i}{6} + (\alpha - i\beta) \frac{\tau}{h^2} \right] \psi_j^n. \end{aligned}$$

This is the CFD scheme for Eq. (8). It possesses second-order accuracy in time and fourth-order accuracy in space. Similarly, Eqs. (10)–(14) can also be solved by this method.

Therefore, we combine the split-step method with the Runge–Kutta method and the CFD scheme to construct new schemes for the 1D, 2D, and 3D CQ CGL equations, which are referred to as the SSRKCFD schemes in this paper.

The SSRKCFD scheme for the 1D CQ CGL equation is formulated as follows:

$$K_1 = \frac{1}{2} [-\delta + (i\alpha_1 + \beta_1)|\psi_j^n|^2 + (i\alpha_2 + \beta_2)|\psi_j^n|^4] \psi_j^n, \quad (26)$$

$$\begin{aligned} K_2 &= \frac{1}{2} [-\delta + (i\alpha_1 + \beta_1)|\psi_j^n + \tau K_1|^2 \\ &+ (i\alpha_2 + \beta_2)|\psi_j^n + \tau K_1|^4] (\psi_j^n + \tau K_1), \end{aligned} \quad (27)$$

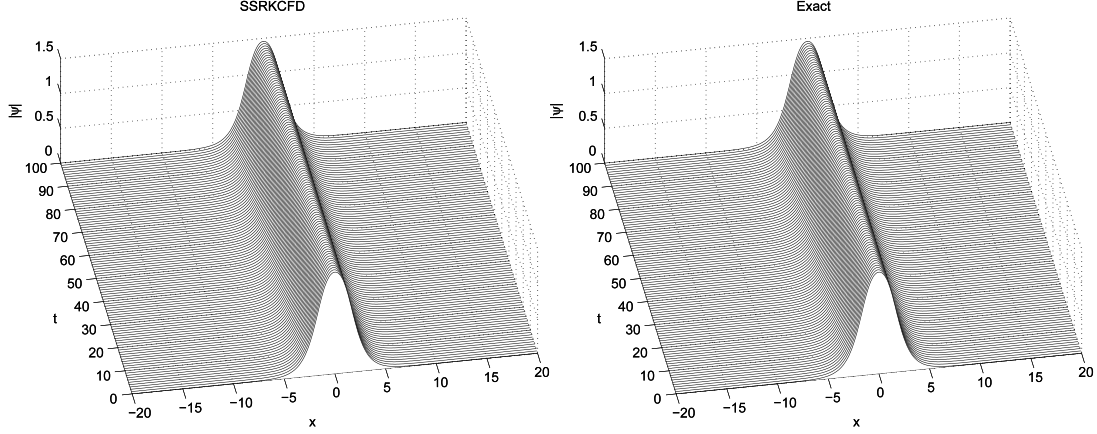


Fig. 2. Numerical simulations of $|\psi|$ for 1D CQ CGL equation. Left: Numerical. Right: Exact.

$$\psi_j^{n+1,1} = \psi_j^n + \frac{\tau}{2}(K_1 + K_2),$$

$$\left[\frac{i}{12} + \frac{1}{2}(\alpha - i\beta) \frac{\tau}{h^2} \right] (\psi_{j+1}^{n+1,2} + \psi_{j-1}^{n+1,2})$$

$$+ \left[\frac{5i}{6} - (\alpha - i\beta) \frac{\tau}{h^2} \right] \psi_j^{n+1,2}$$

$$= \left[\frac{i}{12} - \frac{1}{2}(\alpha - i\beta) \frac{\tau}{h^2} \right] (\psi_{j+1}^{n+1,1} + \psi_{j-1}^{n+1,1})$$

$$+ \left[\frac{5i}{6} + (\alpha - i\beta) \frac{\tau}{h^2} \right] \psi_j^{n+1,1},$$

$$K_1 = \frac{1}{2} \left[-\delta + (i\alpha_1 + \beta_1) |\psi_j^{n+1,2}|^2 + (i\alpha_2 + \beta_2) |\psi_j^{n+1,2}|^4 \right] \psi_j^{n+1,2},$$

$$K_2 = \frac{1}{2} \left[-\delta + (i\alpha_1 + \beta_1) |\psi_j^{n+1,2}|^2 + \tau K_1|^2 + (i\alpha_2 + \beta_2) |\psi_j^{n+1,2}|^4 + \tau K_1|^4 \right] (\psi_j^{n+1,2} + \tau K_1),$$

$$\psi_j^{n+1} = \psi_j^{n+1,2} + \frac{\tau}{2}(K_1 + K_2),$$

for $1 \leq j \leq N$ and $0 \leq n \leq J - 1$.

For $d = 2$, the SSRKCFD method is

$$K_1 = \frac{1}{2} \left[-\delta + (i\alpha_1 + \beta_1) |\psi_{jk}^n|^2 + (i\alpha_2 + \beta_2) |\psi_{jk}^n|^4 \right] \psi_{jk}^n,$$

$$K_2 = \frac{1}{2} \left[-\delta + (i\alpha_1 + \beta_1) |\psi_{jk}^n| + \tau K_1|^2 + (i\alpha_2 + \beta_2) |\psi_{jk}^n + \tau K_1|^4 \right] (\psi_{jk}^n + \tau K_1),$$

$$\psi_{jk}^{n+1,1} = \psi_{jk}^n + \frac{\tau}{2}(K_1 + K_2),$$

$$\left[\frac{i}{12} + \frac{1}{2}(\alpha - i\beta) \frac{\tau}{h^2} \right] (\psi_{j+1,k}^{n+1,2} + \psi_{j-1,k}^{n+1,2})$$

$$+ \left[\frac{5i}{6} - (\alpha - i\beta) \frac{\tau}{h^2} \right] \psi_{jk}^{n+1,2}$$

$$= \left[\frac{i}{12} - \frac{1}{2}(\alpha - i\beta) \frac{\tau}{h^2} \right] (\psi_{j+1,k}^{n+1,1} + \psi_{j-1,k}^{n+1,1})$$

$$+ \left[\frac{5i}{6} + (\alpha - i\beta) \frac{\tau}{h^2} \right] \psi_{jk}^{n+1,1},$$

$$(28) \quad \left[\frac{i}{12} + \frac{1}{2}(\alpha - i\beta) \frac{\tau}{h^2} \right] (\psi_{j,k+1}^{n+1,3} + \psi_{j,k-1}^{n+1,3})$$

$$+ \left[\frac{5i}{6} - (\alpha - i\beta) \frac{\tau}{h^2} \right] \psi_{jk}^{n+1,3}$$

$$= \left[\frac{i}{12} - \frac{1}{2}(\alpha - i\beta) \frac{\tau}{h^2} \right] (\psi_{j,k+1}^{n+1,2} + \psi_{j,k-1}^{n+1,2})$$

$$+ \left[\frac{5i}{6} + (\alpha - i\beta) \frac{\tau}{h^2} \right] \psi_{jk}^{n+1,2},$$

$$(29) \quad K_1 = \frac{1}{2} \left[-\delta + (i\alpha_1 + \beta_1) |\psi_{jk}^{n+1,3}|^2 + (i\alpha_2 + \beta_2) |\psi_{jk}^{n+1,3}|^4 \right] \psi_{jk}^{n+1,3},$$

$$(30) \quad K_2 = \frac{1}{2} \left[-\delta + (i\alpha_1 + \beta_1) |\psi_{jk}^{n+1,3}| + \tau K_1|^2 + (i\alpha_2 + \beta_2) |\psi_{jk}^{n+1,3} + \tau K_1|^4 \right] (\psi_{jk}^{n+1,3} + \tau K_1),$$

$$(31) \quad \psi_{jk}^{n+1} = \psi_{jk}^{n+1,3} + \frac{\tau}{2}(K_1 + K_2),$$

for $1 \leq j, k \leq N$ and $0 \leq n \leq J - 1$.

For the 3D CQ CGL equation, the SSRKCFD method is

$$(41) \quad K_1 = \frac{1}{2} \left[-\delta + (i\alpha_1 + \beta_1) |\psi_{jkl}^n|^2 + (i\alpha_2 + \beta_2) |\psi_{jkl}^n|^4 \right] \psi_{jkl}^n,$$

$$(42) \quad K_2 = \frac{1}{2} \left[-\delta + (i\alpha_1 + \beta_1) |\psi_{jkl}^n| + \tau K_1|^2 + (i\alpha_2 + \beta_2) |\psi_{jkl}^n + \tau K_1|^4 \right] (\psi_{jkl}^n + \tau K_1),$$

$$(43) \quad \psi_{jkl}^{n+1,1} = \psi_{jkl}^n + \frac{\tau}{2}(K_1 + K_2),$$

$$(44) \quad \left[\frac{i}{12} + \frac{1}{2}(\alpha - i\beta) \frac{\tau}{h^2} \right] (\psi_{j+1,kl}^{n+1,2} + \psi_{j-1,kl}^{n+1,2})$$

$$+ \left[\frac{5i}{6} - (\alpha - i\beta) \frac{\tau}{h^2} \right] \psi_{jkl}^{n+1,2}$$

$$= \left[\frac{i}{12} - \frac{1}{2}(\alpha - i\beta) \frac{\tau}{h^2} \right] (\psi_{j+1,kl}^{n+1,1} + \psi_{j-1,kl}^{n+1,1})$$

$$+ \left[\frac{5i}{6} + (\alpha - i\beta) \frac{\tau}{h^2} \right] \psi_{jkl}^{n+1,1},$$

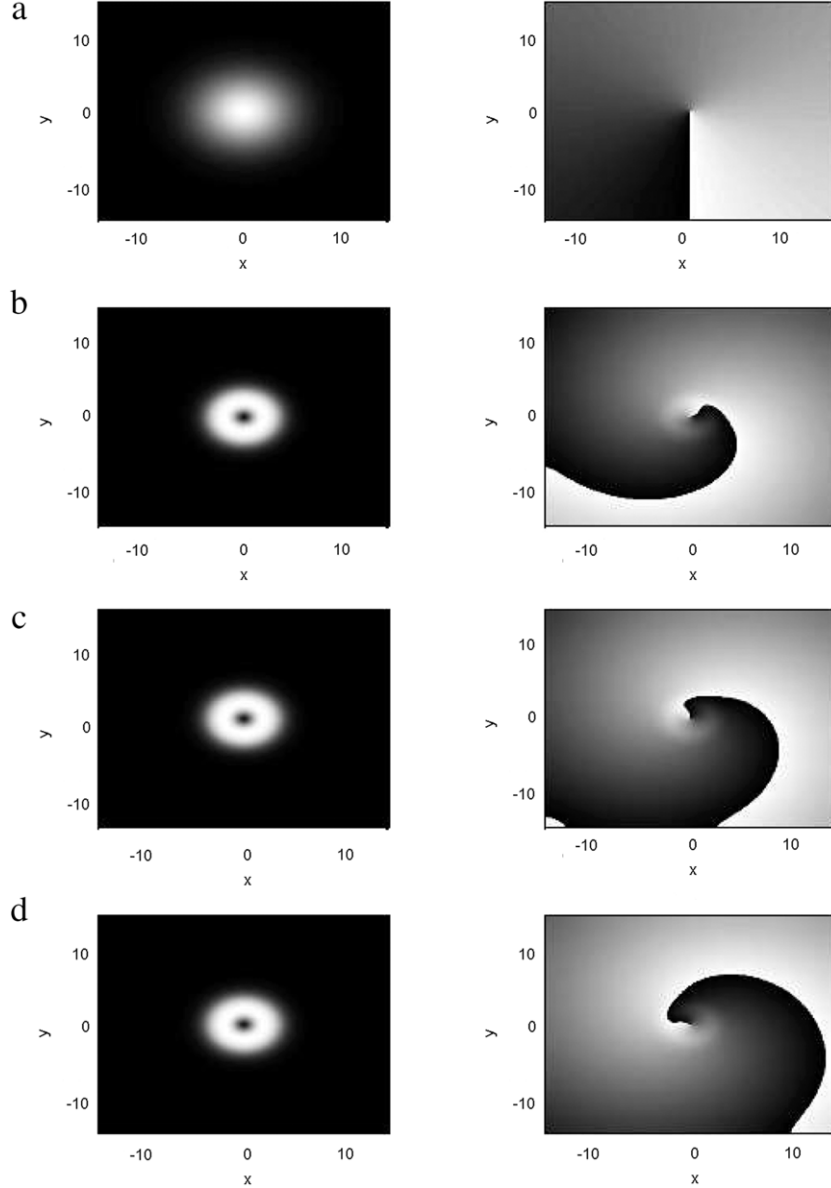


Fig. 3. Numerical simulations of $|\psi|$ for 2D CQ CGL equation with initial condition (50). Left: Amplitude. Right: Phase. (a) $t = 0$, (b) $t = 50$, (c) $t = 100$, (d) $t = 150$.

$$\begin{aligned} & \left[\frac{i}{12} + \frac{1}{2}(\alpha - i\beta) \frac{\tau}{h^2} \right] (\psi_{j,k+1,l}^{n+1,3} + \psi_{j,k-1,l}^{n+1,3}) \\ & + \left[\frac{5i}{6} - (\alpha - i\beta) \frac{\tau}{h^2} \right] \psi_{jkl}^{n+1,3} \\ & = \left[\frac{i}{12} - \frac{1}{2}(\alpha - i\beta) \frac{\tau}{h^2} \right] (\psi_{j,k+1,l}^{n+1,2} + \psi_{j,k-1,l}^{n+1,2}) \\ & + \left[\frac{5i}{6} + (\alpha - i\beta) \frac{\tau}{h^2} \right] \psi_{jkl}^{n+1,2}, \end{aligned} \quad (45)$$

$$\begin{aligned} & \left[\frac{i}{12} + \frac{1}{2}(\alpha - i\beta) \frac{\tau}{h^2} \right] (\psi_{jk,l+1}^{n+1,4} + \psi_{jk,l-1}^{n+1,4}) \\ & + \left[\frac{5i}{6} - (\alpha - i\beta) \frac{\tau}{h^2} \right] \psi_{jkl}^{n+1,4} \\ & = \left[\frac{i}{12} - \frac{1}{2}(\alpha - i\beta) \frac{\tau}{h^2} \right] (\psi_{jk,l+1}^{n+1,3} + \psi_{jk,l-1}^{n+1,3}) \end{aligned}$$

$$+ \left[\frac{5i}{6} + (\alpha - i\beta) \frac{\tau}{h^2} \right] \psi_{jkl}^{n+1,3}, \quad (46)$$

$$\begin{aligned} K_1 &= \frac{1}{2} \left[-\delta + (i\alpha_1 + \beta_1) |\psi_{jkl}^{n+1,4}|^2 \right. \\ &\quad \left. + (i\alpha_2 + \beta_2) |\psi_{jkl}^{n+1,4}|^4 \right] \psi_{jkl}^{n+1,4}, \end{aligned} \quad (47)$$

$$\begin{aligned} K_2 &= \frac{1}{2} \left[-\delta + (i\alpha_1 + \beta_1) |\psi_{jkl}^{n+1,4}|^2 + \tau K_1 \right]^2 \\ &\quad + (i\alpha_2 + \beta_2) |\psi_{jkl}^{n+1,4} + \tau K_1|^4 (\psi_{jkl}^{n+1,4} + \tau K_1), \end{aligned} \quad (48)$$

$$\psi_{jkl}^{n+1} = \psi_{jkl}^{n+1,4} + \frac{\tau}{2}(K_1 + K_2), \quad (49)$$

for $1 \leq j, k, l \leq N$ and $0 \leq n \leq J - 1$.

3. Numerical experiments

Various tests are carried out to examine the numerical performance of the SSRKCFD method. Throughout the computations, the

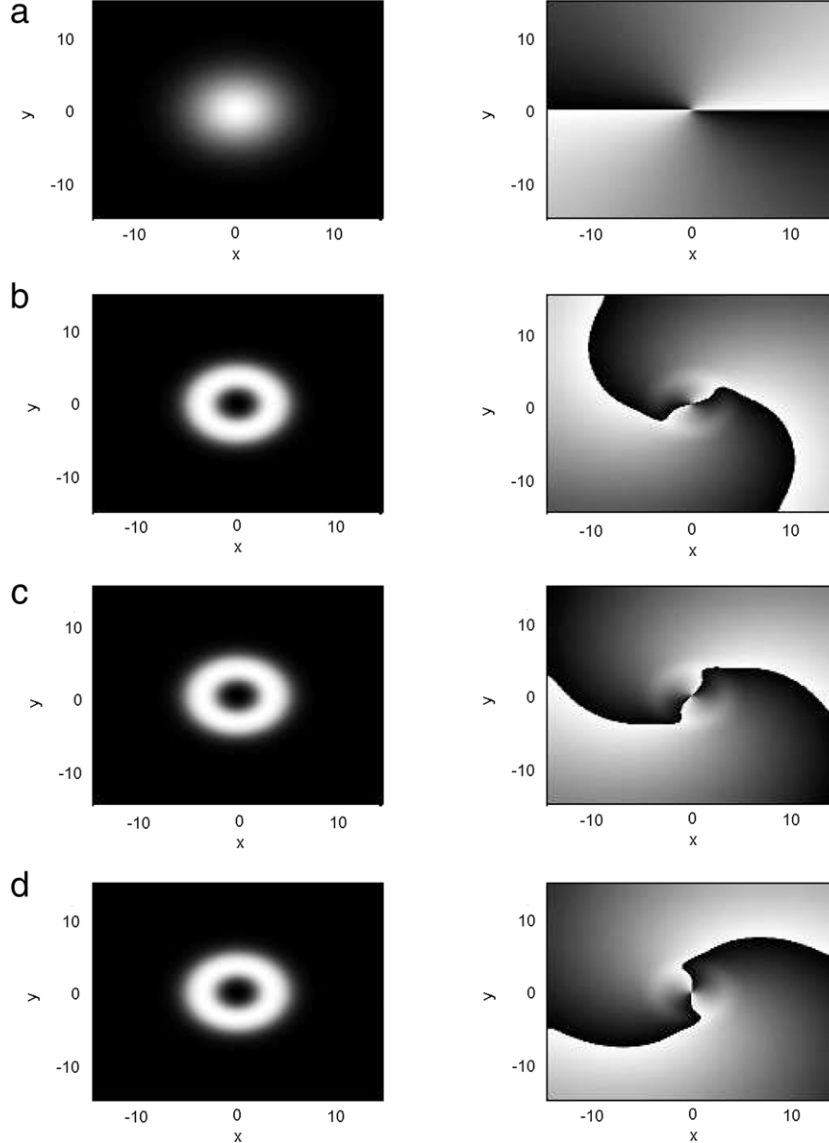


Fig. 4. Numerical simulations of $|\psi|$ for 2D CQ CGL equation with initial condition (51). Left: Amplitude. Right: Phase. (a) $t = 0$, (b) $t = 50$, (c) $t = 100$, (d) $t = 150$.

maximum norm error is defined as

$$\|\epsilon\|_\infty = \max_n \|\epsilon^n\|_\infty = \max_{n, \mathbf{k}} \|\psi_{\mathbf{k}}^n - \psi(\mathbf{x}_k, t_n)\|_\infty.$$

Example 1. Set $\alpha = \beta = 1$, $\alpha_1 = \alpha_2 = -1$, and $\beta_1 = \beta_2 = -1/2$. The CQ CGL equation (1) has a plane wave solution:

$$\psi(\mathbf{x}, t) = ae^{i(\xi\mathbf{x} - \omega t)},$$

where $a = 1$, $\xi = \pi/3$, $\omega = (1 - i)\xi^2 - i\delta + 2 - i$, and

$$\delta = \begin{cases} -1 - \xi^2 i, & d = 1, \\ -1 - 2\xi^2 i, & d = 2, \\ -1 - 3\xi^2 i, & d = 3. \end{cases}$$

Periodic boundary conditions are used, and the problem is solved within $(\mathbf{x}, t) \in [0, 6]^d \times [0, 1]$. Take $\tau = h^2$. Curves of convergence rates of the SSRKCFD schemes for the 1D, 2D, and 3D CQ CGL equations are plotted in Fig. 1. As the curves are almost straight lines and their slopes approximate to 4, the proposed schemes are convergent of second-order in time, and fourth-order in space.

Example 2. The NLS problems in 1D, 2D, and 3D [21] are calculated, and the SSRKCFD method is compared with the SSCFD [22]

Table 1
Maximum errors of three schemes for 1D, 2D, and 3D NLS problems.

	SSRKCFD	SSCFD	SSFD
1D	5.74e-4	1.15e-4	5.14e-2
2D	3.31e-4	2.31e-4	1.02e-1
3D	1.24e-4	3.46e-4	1.54e-1

and the SSFD [21] methods, where the 1D SSCFD scheme in [22] is extended for the multi-dimensional problems. These equations are solved within $(\mathbf{x}, t) \in [0, 2\pi]^d \times [0, 50]$. Maximum errors, i.e. $\|\epsilon\|_\infty$, are listed in Table 1. One can conclude that the SSRKCFD method is more efficient than the SSFD one, and comparable to the SSCFD approach.

Example 3. The cubic CGL equation:

$$i\frac{\partial\psi}{\partial t} + \frac{1}{2}\frac{\partial^2\psi}{\partial x^2} + |\psi|^2\psi = i\delta\psi + i\beta\frac{\partial^2\psi}{\partial x^2} + i\epsilon|\psi|^2\psi,$$

has a solution of the following form [5,6]:

$$\psi(x, t) = a(x) \exp\{id \ln[a(x)] - i\omega t\},$$

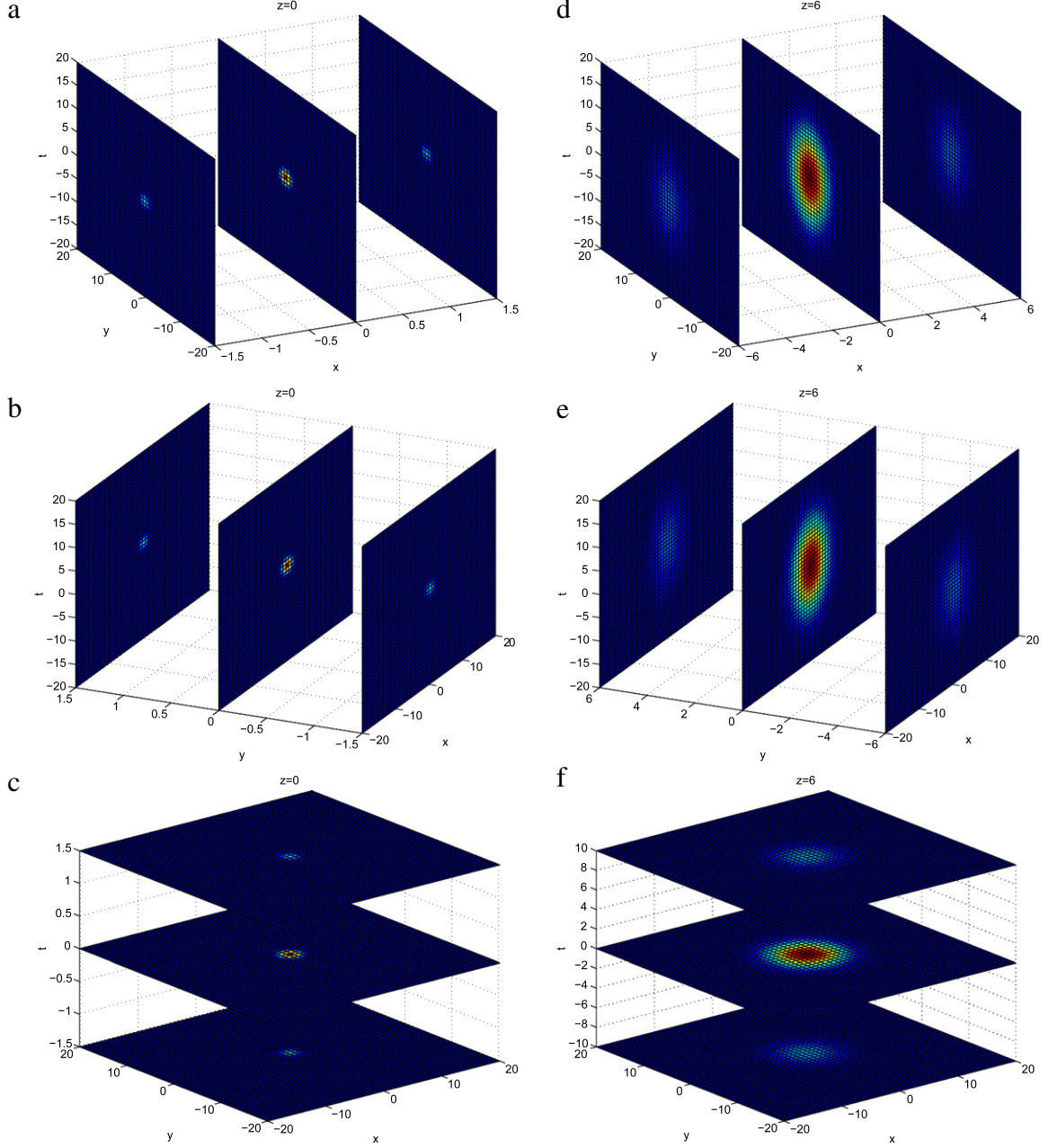


Fig. 5. (Color online) Numerical simulations of $|\psi|$ for 3D CQ CGL equation with initial condition (52). Left: $z = 0$. Right: $z = 6$. (a) slices at $x = -1.5, 0, 1.5$; (b) slices at $y = -1.5, 0, 1.5$; (c) slices at $t = -1.5, 0, 1.5$; (d) slices at $x = -6, 0, 6$; (e) slices at $y = -6, 0, 6$; (f) slices at $t = -10, 0, 10$.

Table 2
Errors of two schemes for 1D cubic CGL equation.

t	SSRKCFD	SSCFD
1	3.10e-5	8.26e-6
10	2.95e-4	8.95e-6
20	4.91e-4	9.82e-5
40	5.73e-4	6.25e-4
60	2.45e-4	1.58e-3
80	4.97e-4	2.97e-3
100	1.64e-3	4.79e-3

where $(x, t) \in [-20, 20] \times [0, 100]$, $\delta = 0$, $\beta = 0.3$, and

$$a(x) = F \operatorname{sech}(x), \quad F^2 = \frac{d\sqrt{1+4\beta^2}}{2\epsilon}, \quad d = \frac{\sqrt{1+4\beta^2}-1}{2\beta},$$

$$\epsilon = \frac{\beta(3\sqrt{1+4\beta^2}-1)}{2(2+9\beta^2)}, \quad \omega = -\frac{d(1+4\beta^2)}{2\beta}.$$

The SSRKCFD and the SSCFD schemes are applied, and the errors, i.e. $\|\epsilon^n\|_\infty$, are given in Table 2. The SSRKCFD method is still comparable to the SSCFD one.

Example 4. The CQ CGL equation [5,6]:

$$\begin{aligned} & i \frac{\partial \psi}{\partial t} + \frac{1}{2} \frac{\partial^2 \psi}{\partial x^2} + |\psi|^2 \psi \\ & = i\delta \psi + i\beta \frac{\partial^2 \psi}{\partial x^2} + i\epsilon |\psi|^2 \psi + i\mu |\psi|^4 \psi - \nu |\psi|^4 \psi \end{aligned}$$

has a stationary pulse solution as follows:

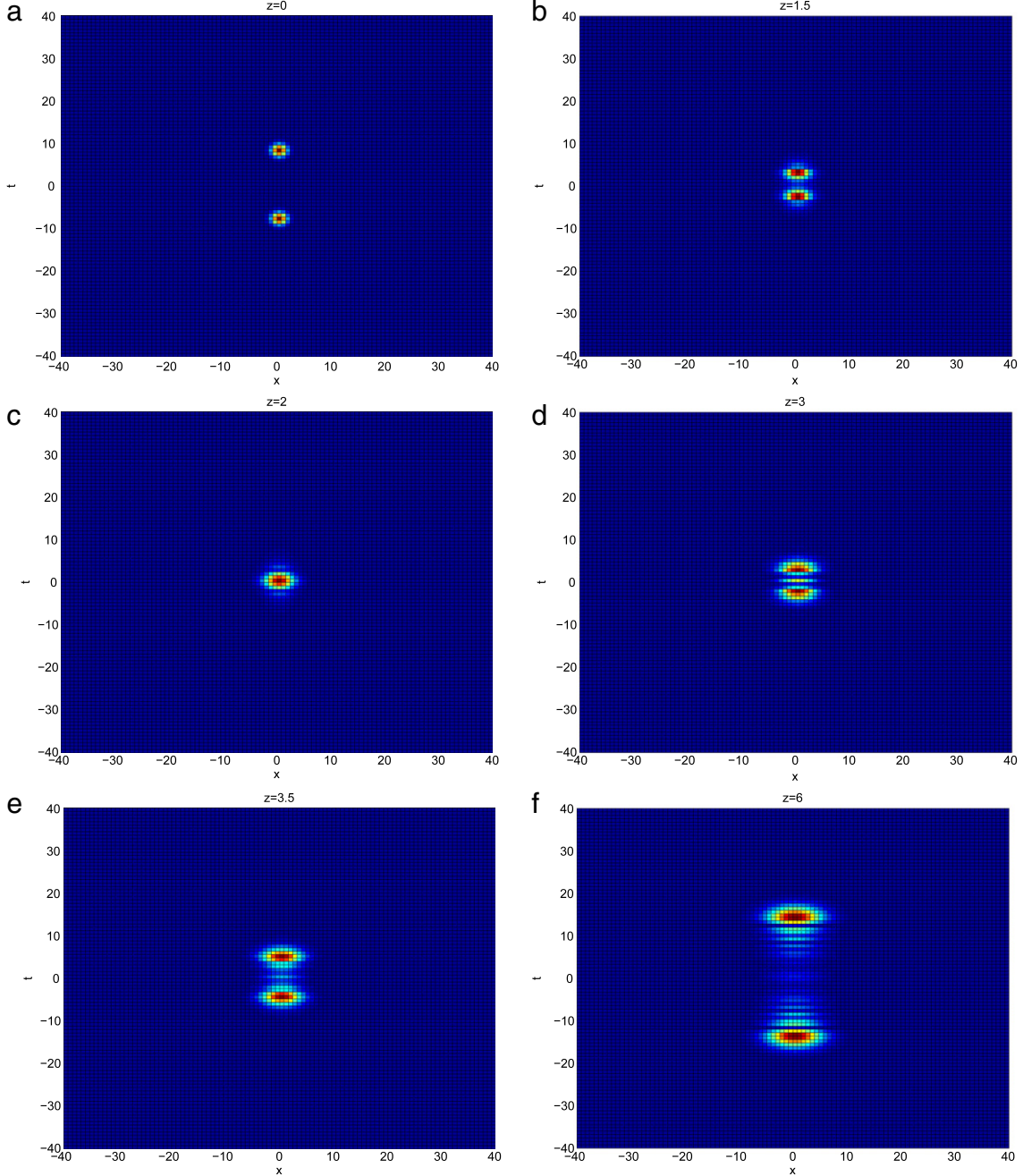


Fig. 6. (Color online) Slices of $|\psi|$ at $y = 0$ for 3D CQ CGL equation. (a) $z = 0$, (b) $z = 1.5$, (c) $z = 2$, (d) $z = 3$, (e) $z = 3.5$, (f) $z = 6$.

$$\psi(x, t) = a(x) \exp \{id \ln[a(x)] - i\omega t\},$$

where $(x, t) \in [-20, 20] \times [0, 100]$, $\delta = 0$, $\beta = 0.3$, $\nu = -0.3$, and

$$\begin{aligned} a &= \sqrt{f}, \quad f(x) = \frac{3d(1+4\beta^2)}{(2\beta-\epsilon)+S \cdot \cosh(2x)}, \\ S &= \sqrt{(2\beta-\epsilon)^2 + \frac{18d^2\nu(1+4\beta^2)^2}{8\beta d - d^2 + 3}}, \\ d &= \frac{\sqrt{1+4\beta^2}-1}{2\beta}, \quad \epsilon = \frac{\beta(3\sqrt{1+4\beta^2}-1)}{2(2+9\beta^2)}, \\ \omega &= -\frac{d(1+4\beta^2)}{2\beta}, \end{aligned}$$

$$\mu = \frac{-\nu [d(12\epsilon\beta^2 + 4\epsilon - 2\beta) - 2\beta(\epsilon - 2\beta)]}{d(2\epsilon\beta - 16\beta^2 - 3) + \epsilon - 2\beta}.$$

The SSRKCFD scheme is performed, and the result is plotted in Fig. 2. The numerical surface agrees with the exact one, so the numerical method is reliable and efficient.

Example 5. Consider the 2D CQ CGL equation [7] as follows:

$$\begin{aligned} i \frac{\partial \psi}{\partial t} + i\delta \psi + \left(\frac{1}{2} - i\beta\right) \left(\frac{\partial^2 \psi}{\partial x^2} + \frac{\partial^2 \psi}{\partial y^2}\right) \\ + (1-i\epsilon)|\psi|^2\psi - (\nu - i\mu)|\psi|^4\psi = 0. \end{aligned}$$

Take $\beta = 0.5$, $\delta = 0.5$, $\nu = 0.1$, $\mu = 1$ and $\epsilon = 2.5$. Two spiral solitons are simulated by the SSRKCFD scheme. The two initial

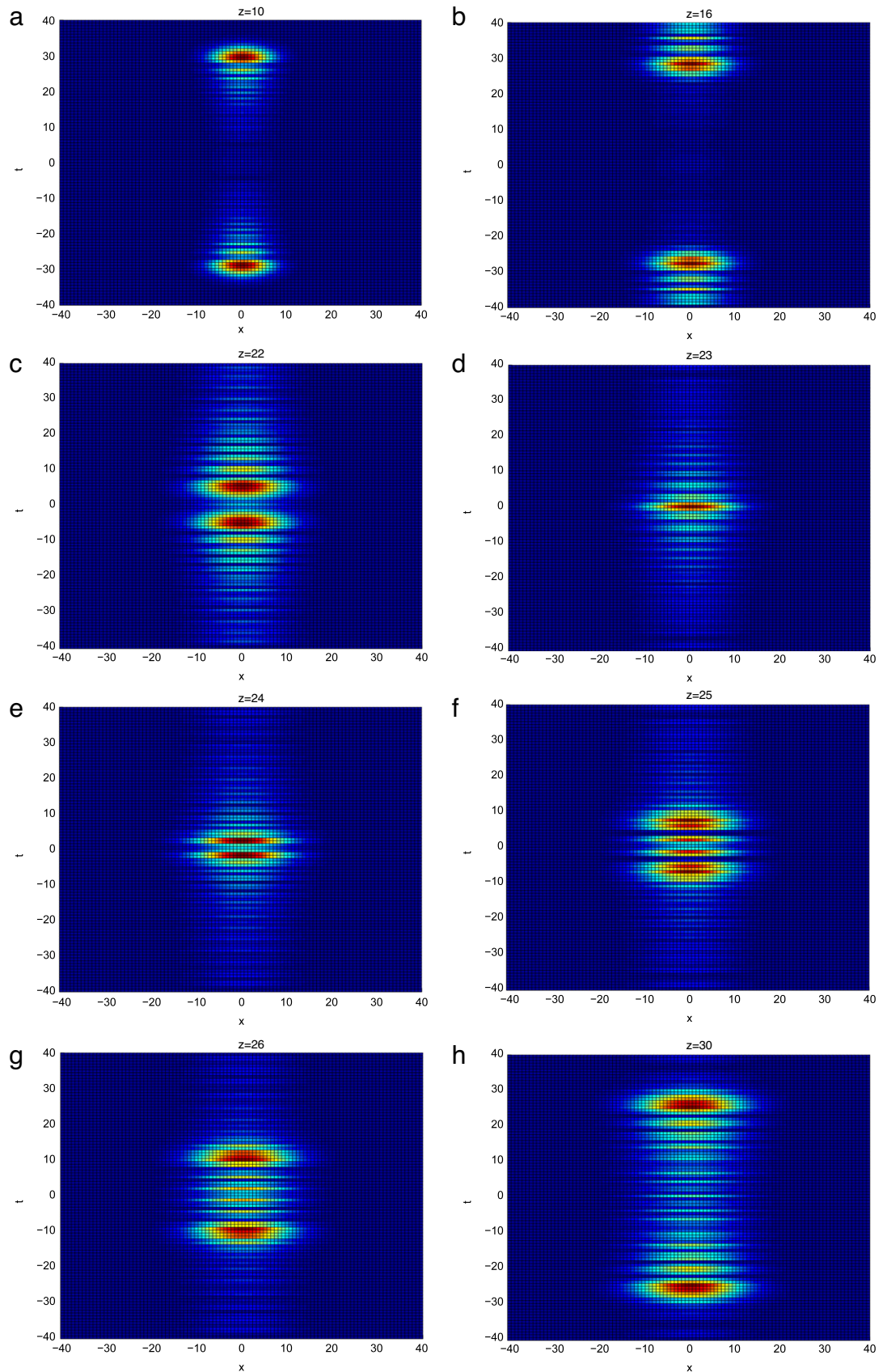


Fig. 7. (Color online) Slices of $|\psi|$ at $y = 0$ for 3D CQ CGL equation. (a) $z = 10$, (b) $z = 16$, (c) $z = 22$, (d) $z = 23$, (e) $z = 24$, (f) $z = 25$, (g) $z = 26$, (h) $z = 30$.

distributions are respectively given as

$$\psi(x, y, 0) = \begin{cases} 1.6 \exp\left(-\frac{x^2 + y^2}{25}\right) \frac{x + iy}{\sqrt{x^2 + y^2}}, & (x, y) \neq (0, 0), \\ 0, & (x, y) = (0, 0). \end{cases} \quad (50)$$

and

$$\psi(x, y, 0) = \begin{cases} 1.6 \exp\left(-\frac{x^2 + y^2}{25}\right) \frac{x^2 - y^2 + 2ixy}{x^2 + y^2}, & (x, y) \neq (0, 0), \\ 0, & (x, y) = (0, 0). \end{cases} \quad (51)$$

Figs. 3 and 4 show the transformations of the amplitude and phase of each soliton with various values of t .

Example 6. Consider the following 3D CQ CGL equation [10]–[12]:

$$i \frac{\partial \psi}{\partial z} + \left(\frac{1}{2} - i\beta\right) \left(\frac{\partial^2 \psi}{\partial x^2} + \frac{\partial^2 \psi}{\partial y^2} \right) + \left(\frac{D}{2} - i\gamma\right) \frac{\partial^2 \psi}{\partial t^2} + [i\delta + (1 - i\epsilon)|\psi|^2 - (\nu - i\mu)|\psi|^4]\psi = 0.$$

In nonlinear optics, this equation describes the model of a bulk optical medium, where ψ is the local amplitude of a electromagnetic wave propagating along axis z . The transverse coordinates are x and y , and t is a variable related to time. $\beta \geq 0$ is the diffusivity in the transverse plane which is necessary for the stability of solitons. Setting $\gamma = 0$ will make the solitons collide. Set $\beta = 0.5$, $D = 1$, $\delta = 0.4$, $\epsilon = 2.3$, $\mu = 1$ and $\nu = 0.1$.

Firstly, the input pulse is given as

$$\psi(z = 0, x, y, t) = \exp\left[-\frac{1}{2}(x^2 + y^2 + t^2)\right], \quad (52)$$

and numerical simulations of $|\psi|$ at $z = 0$ and $z = 6$ are given in Fig. 5. The wave is dissipating. The value of $|\psi|$ at the center $(z, 0, 0, 0)$ is vanishing: $|\psi| = 1$ at $z = 0$, while $|\psi| = 5.7 \times 10^{-3}$ at $z = 6$.

Next, the following initial condition is considered:

$$\psi(z = 0, x, y, t) = \exp\left\{-\frac{1}{2}[x^2 + y^2 + (t + 8)^2] + i5z\right\} + \exp\left\{-\frac{1}{2}[x^2 + y^2 + (t - 8)^2] - i5z\right\}, \quad (53)$$

where two initial solitons of (52) are separated by a temporal distance 16, and multiplied respectively by $\exp(\pm i5z)$ to set them in motion [11,12]. Collisions at various values of z are plotted in Figs. 6 and 7. At first, the two waves are positioned at $t = \pm 8$, respectively. They approach each other, and hit at $z = 2$. Then they separate. From $z = 10$ to $z = 16$, the two waves go on to move to the boundary, and rebound. Then they approach each other again, and collide at $z = 23$ for the second time. After that they separate, and move to the boundary again. During the whole process, they are dissipating themselves. One can predict that they will rebound and collide again and again until they disappear. The collisions are quasi-elastic.

4. Conclusion

SSRKCFD schemes are constructed for the 1D, 2D, and 3D CQ CGL equations. Firstly, the original equations are separated into

two nonlinear subproblems and one or several 1D linear equations. For the linear subproblems, the compact finite difference schemes are applied. Since the nonlinear subproblems cannot be solved exactly, the second-order Runge–Kutta method is utilized, and the accuracy order is not reduced. These schemes are convergent of order $O(t^2 + h^4)$, which is verified numerically. The SSRKCFD method is compared with the SSCFD and the SSFD method for the NLS equations and the cubic CGL equation. The present SSRKCFD method is more efficient than the SSFD one, and comparable to the SSCFD method. As the SSFD and the SSCFD methods are not suitable for the CQ CGL equation, the SSRKCFD method is taken into account. Numerical experiments are carried out to test the performance of the SSRKCFD method for the 1D, 2D, and 3D CQ CGL equations. It is shown from all the numerical tests that, the proposed SSRKCFD method is efficient and reliable.

References

- [1] I.S. Aranson, L. Kramer, The world of the complex Ginzburg–Landau equation, Rev. Modern Phys. 74 (2002) 99–143.
- [2] N. Akhmediev, A. Ankiewicz (Eds.), Dissipative Solitons, Springer, Berlin, 2005.
- [3] N. Akhmediev, A. Ankiewicz (Eds.), Dissipative Solitons: From Optics to Biology and Medicine, Springer, Berlin, 2008.
- [4] V.I. Petviashvili, A.M. Sergeev, Spiral solitons in active media with an excitation threshold, Sov. Phys. Dokl. 29 (6) (1984) 493–495.
- [5] N. Akhmediev, V.V. Afanasjev, Novel arbitrary-amplitude soliton solutions of the cubic-quintic complex Ginzburg–Landau equation, Phys. Rev. Lett. 75 (12) (1995) 2320–2323.
- [6] N.N. Akhmediev, V.V. Afanasjev, Singularities and special soliton solutions of the cubic-quintic complex Ginzburg–Landau equation, Phys. Rev. E 53 (1) (1996) 1190–1201.
- [7] L.-C. Crasovan, B.A. Malomed, D. Mihalache, Stable vortex solitons in the two-dimensional Ginzburg–Landau equation, Phys. Rev. E 63 (2000) 016605.
- [8] Y. Shi, Z. Dai, D. Li, Application of Exp-function method for 2D cubic-quintic Ginzburg–Landau equation, Appl. Math. Comput. 210 (2009) 269–275.
- [9] V. Skarka, N.B. Aleksić, Stability criterion for dissipative soliton solutions of the one-, two-, and three-dimensional complex cubic-quintic Ginzburg–Landau equations, Phys. Rev. Lett. 96 (2006) 013903.
- [10] D. Mihalache, D. Mazilu, F. Lederer, et al., Stability of dissipative optical solitons in the three-dimensional cubic-quintic Ginzburg–Landau equation, Phys. Rev. A 75 (2007) 033811.
- [11] D. Mihalache, D. Mazilu, F. Lederer, et al., Collisions between coaxial vortex solitons in the three-dimensional cubic-quintic complex Ginzburg–Landau equation, Phys. Rev. A 77 (2008) 033817.
- [12] D. Mihalache, D. Mazilu, Three-dimensional Ginzburg–Landau solitons: collision scenarios, Rom. Rep. Phys. 61 (2) (2009) 175–189.
- [13] J.M. Soto-Crespo, N.N. Akhmediev, V.V. Afanasjev, Stability of the pulselike solutions of the quintic complex Ginzburg–Landau equation, J. Opt. Soc. Am. B 13 (7) (1996) 1439–1449.
- [14] I. Towers, A.B. Buryak, R.A. Sammut, et al., Stability of spinning ring solitons of the cubic-quintic nonlinear Schrödinger equation, Phys. Lett. A 288 (2001) 292–298.
- [15] G.P. Agrawal, Nonlinear Fiber Optics, fourth ed., World Publishing Corporation, Beijing, 2009.
- [16] N.N. Yanenko, The Method of Fractional Steps: The Solution of Problems of Mathematical Physics in Several Variables, Springer, New York, 1971.
- [17] S. Yu, S. Zhao, G.W. Wei, Local spectral time splitting method for first- and second-order partial differential equations, J. Comput. Phys. 206 (2005) 727–780.
- [18] T.R. Taha, M.J. Ablowitz, Analytical and numerical aspects of certain nonlinear evolution equations. II. Numerical, nonlinear Schrödinger equation, J. Comput. Phys. 55 (1984) 203–230.
- [19] W. Bao, S. Jin, P.A. Markowich, On time-splitting spectral approximations for the Schrödinger equation in the semiclassical regime, J. Comput. Phys. 175 (2002) 487–524.
- [20] W. Bao, D. Jaksch, An explicit unconditionally stable numerical method for solving damped nonlinear Schrödinger equations with a focusing nonlinearity, SIAM J. Numer. Anal. 41 (4) (2003) 1406–1426.
- [21] H. Wang, Numerical studies on the split-step finite difference method for nonlinear Schrödinger equations, Appl. Math. Comput. 170 (2005) 17–35.
- [22] M. Dehghan, A. Taleei, A compact split-step finite difference method for solving the nonlinear Schrödinger equations with constant and variable coefficients, Comput. Phys. Comm. 181 (2010) 43–51.

- [23] D. Goldman, L. Sirovich, A novel method for simulating the complex Ginzburg–Landau equation, *Quart. Appl. Math.* 53 (2) (1995) 315–333.
- [24] Y. Zhang, W. Bao, Q. Du, Numerical simulation of vortex dynamics in Ginzburg–Landau–Schrödinger equation, *European J. Appl. Math.* 18 (2007) 607–630.
- [25] H. Wang, An efficient Chebyshev–Tau spectral method for Ginzburg–Landau–Schrödinger equations, *Comput. Phys. Comm.* 181 (2010) 325–340.
- [26] P. Degond, S. Jin, M. Tang, On the time splitting spectral method for the complex Ginzburg–Landau equation in the large time and space scale limit, *SIAM J. Sci. Comput.* 30 (5) (2008) 2466–2487.
- [27] Q. Xu, Q. Chang, Difference methods for computing the Ginzburg–Landau equation in two dimensions, *Numer. Methods Partial Differential Equations* 27 (3) (2011) 507–528.
- [28] G. Wainblat, B.A. Malomed, Interactions between two-dimensional solitons in the diffractive-diffusive Ginzburg–Landau equation with the cubic-quintic nonlinearity, *Phys. D* 238 (2009) 1143–1151.
- [29] G. Strang, On the construction and comparison of difference schemes, *SIAM J. Numer. Anal.* 5 (3) (1968) 506–517.
- [30] R.L. Burden, J.D. Faires, *Numerical Analysis*, seventh ed., Higher Education Press, Beijing, 2002.